Experimental study of underground coal gasification (UCG) of a high-rank coal using atmospheric and high-pressure conditions in an ex-situ reactor

Renato Zagorščak [a,*], Sivachidambaram Sadasivam [a], Hywel Rhys Thomas [a], Krzysztof

Stańczyk [b], Krzysztof Kapusta [b]

[a] *Geoenvironmental Research Centre (GRC), School of Engineering, Cardiff University, The Queen's Buildings, The Parade, Cardiff, CF24 3AA, United Kingdom*

[b] *Główny Instytut Górnictwa (Central Mining Institute), Plac Gwarków 1, 40-166 Katowice, Poland*

Abstract:

This paper presents the results of an extensive experimental analysis of underground coal gasification (UCG) using large bulk samples in an ex-situ reactor under atmospheric and high-pressure (30 bar) conditions. The high-rank coal obtained from the South Wales (UK) coalfield is employed for that purpose. The aim of this investigation is to define the gas production rates, gas composition, gas calorific value, process energy efficiency and temperature changes within the UCG reactor during the gasification process based on the pre-defined reactants and flow rates. Two UCG trials, each lasting 105 hours, consisted of six stages where the influences of oxygen, water, air and oxygen enriched air (OEA) under different flow conditions on the gasification process were investigated. Based on the results of two multi-day experiments, it is demonstrated that the gasification under high pressure conditions produces syngas with higher average calorific value (8.49 MJ/Nm^3) in comparison to syngas produced at atmospheric pressure conditions (6.92 MJ/Nm^3). Hence, the overall energy efficiency of the high-pressure experiment is higher compared to the atmospheric pressure test, i.e. 57.67% compared to 51.72%. This is related to the fact that the high-pressure gasification produces more methane (11.97 vol.%) than the atmospheric pressure gasification (2.30 vol.%). Under elevated pressure, the temperatures recorded in the roof strata are about 100°C higher compared to the UCG process under atmospheric pressure conditions. This work provides new insights into the gasification of carbon-rich coals subject to different gasification regimes and pressures.

Keywords:

Underground coal gasification; coal; high pressure; syngas; anthracite; in-situ laboratory tests

* Corresponding author:
Renato Zagorščak
ZagorscakR@cardiff.ac.uk
+44 (0) 29208 76264
Geoenvironmental Research Centre (GRC)
School of Engineering, Cardiff University
The Queen's Buildings
The Parade
CF24 3AA
Cardiff
United Kingdom

1. Introduction

Climate change represents a great threat to human society and the planet and there is an urgent need to limit the global warming to 1.5°C above pre-industrial levels by adopting greenhouse gas emissions pathways and low-carbon technologies to achieve a cost-effective transition [1]. On a global scale, it will be necessary to remove around 810 Gt of CO_2 by 2100 to achieve such target [2]. However, the rising incomes and an extra 1.7 billion people, predominantly in the urban areas of the developing economies, is expected to push up the global energy demand by more than a quarter to 2040 [3]. As the fossil fuels will remain a major part of the global energy mix accounting for around 40% of primary energy use in 2050 [4], the environmental footprint of the existing and emerging technologies must therefore be reduced and kept to a minimum.

One of the technologies that offer a prospect towards the transition in the low-carbon future is the Underground Coal Gasification (UCG) through which deep coal deposits can be utilised for the in-situ production of a synthetic gas predominantly consisting of hydrogen, methane, carbon monoxide and carbon dioxide [5, 6]. As the coal reserves significantly exceed those of oil and gas, and less than one sixth of the world's coal is economically accessible, UCG offers a possibility to utilise such reserves in a more environmentally safer way than the conventional mining techniques by eliminating mine safety issues, surface damage and solid waste at the surface [7]. Furthermore, potential UCG sites are often in the vicinity of geological formations suitable for CO_2 sequestration or enhanced oil recovery in which the CO_2 generated by UCG could be stored [7, 8].

UCG has a history of development around the world [8], with the majority of field trials being conducted in the United States [9-11], European Union [12-14], China [15], Australia [16] and the former Soviet Union [17]. Most trials have demonstrated that the UCG can be successfully conducted and that under specific geological and thermodynamic conditions, environmental impact can be minimised. However, despite its potential and over a century of development, UCG has still not been commercialised.

66 The UCG provides a potential mean for the recovery of energy from deep coal deposits that are

67 uneconomic to mine. Hence, conducting experimental investigations on coals of different rank under

68 elevated pressures and using a range of gasification reagents under different flow regimes is required.

69 This would provide further understanding of the UCG technology and its impact on the environment

70 under relevant conditions. Up to date, a large amount of experimental research work has been

71 conducted on bituminous, sub-bituminous and lignite coals predominantly under atmospheric

72 pressure conditions [18-25]. Only a small number of researchers performed gasification experiments

73 under elevated pressures, however, on low rank coals [26, 27] or in small-scale [28, 29]. Hence, as the

74 composition of the product gas and the efficiency of the UCG process depend on the thermodynamic

75 conditions of the process, the coal composition as well as the gasifying agent used, further information

76 of both atmospheric and high pressure gasification processes in large-scale obtained during injection

77 of different gasification reagents on carbon-rich coals is required.

78 This study deals with the large-scale ex-situ gasification of high-rank coal obtained from the South

79 Wales coalfield, UK both at atmospheric and high-pressure (30 bar) conditions using a range of

80 gasification reagents under different flow regimes. Prior to the gasification experiments, the coal was

81 characterised using Proximate and Ultimate analyses, sulphur form analysis and petrographic

82 composition. Two multi-days trials, each lasting 105 hours, were carried out using artificial coal seams

83 each with a mass of 650 kg, as described below. The experiments involved testing the influence of

84 gasifying medium (oxygen, water, air and oxygen enriched air – OEA) under different flow and

85 pressure conditions on the syngas composition and overall process efficiency. Furthermore,

86 temperature changes within the reactor were continuously monitored throughout each experiment.

87 This work provides new insights into the gasification of high-rank coal as well as the coal from the

88 South Wales coalfield demonstrating its applicability for UCG technology.

89 ## 2. Experimental setup and methodology

90 ### 2.1.   Ex-situ high-pressure UCG facility

The experimental simulations of UCG process involved the use of large-scale laboratory facilities of Główny Instytut Górnictwa's (GIG) Clean Coal Technology Centre located at Experimental Mine "Barbara" in Mikołów, Poland [26, 27]. The gasification chamber used as a part of the ex-situ surface installation enables simulations of UCG in an artificial coal seam (max. seam length 3.5 m, cross section 0.41×0.41 m) where gasification media like oxygen, air, steam and hydrogen can be used (Fig. 1). Maximum gasification pressure and temperature that can be achieved and controlled within the chamber are 50 bar and 1600 °C, respectively. Concentrations of the main gaseous components were analysed using gas chromatography technique where the product gas was sampled every 30 minutes. Concentrations of CH_4, H_2, CO, CO_2, C_2H_6, N_2 and H_2S within the gas mixture were determined. Distribution of temperature during the gasification process was controlled by ten high-temperature thermocouples, i.e. five placed in the gasification channel and five in the roof strata (Fig. 2a). The first thermocouples (T2 and T9) were placed 0.5 m away from the face of the coal seam (inlet of the reactor). Remaining thermocouples (T3-T6 and T10-T13) were then spaced 0.5 m apart. In order to protect them from direct contact with oxidizers, the thermocouples were placed in the insulating layer, approximately 2 cm from the bottom and roof of the artificial coal seam (Fig. 2b). Further details on the experimental facility can be found elsewhere [26, 27].
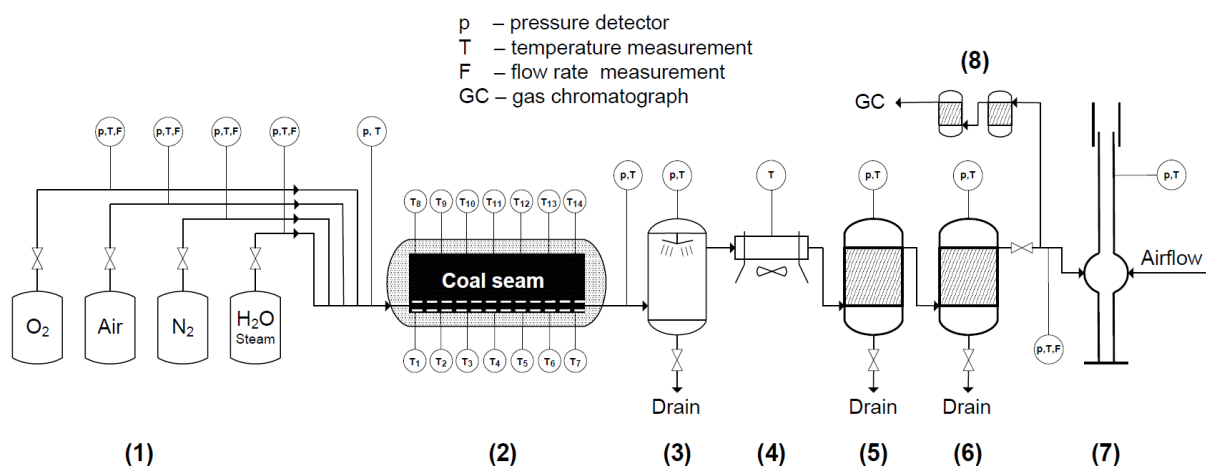

Fig. 1. Scheme of the ex-situ high-pressure UCG installation: (1) compressed reagents, (2) pressure reactor, (3) wet scrubber for gas cleaning, (4) air cooler, (5, 6) gas separators, (7) thermal combustor, (8) gas treatment module prior to GC analysis.
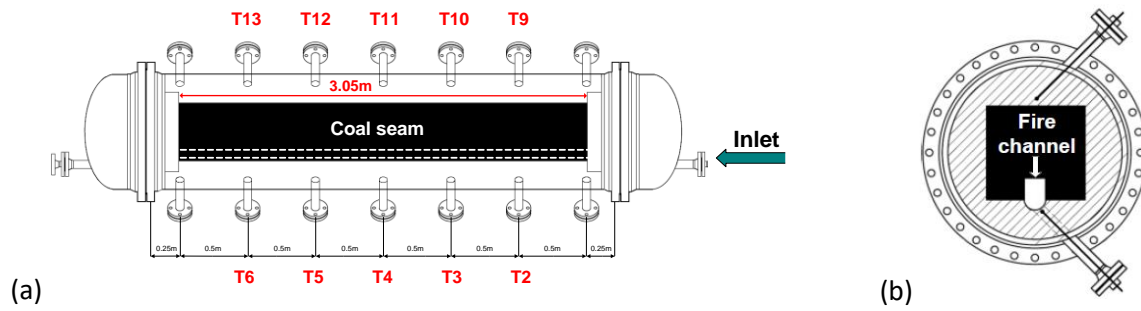
Fig. 2. (a) Pressure reactor side cross-section, (b) pressure reactor longitudinal cross-section.

2.2. Sample preparation and characterisation

Six large coal blocks were collected from an open cast coal mine in the South Wales coalfield, close to Merthyr Tydfil, UK. The coal blocks belong to the Gellideg coal seam and were obtained from 135 m below the original ground level, i.e. 262 m above ordnance datum. Upon extraction, the coal blocks were wrapped in cling film to minimize the oxidation of the coal surfaces and preserve chemical and physical properties, and then put in wooden crates to be transported to the laboratory at GIG for further analysis and preparation. Upon arrival to GIG, raw coal samples were processed using a diamond rope saw to create a continuous artificial coal seam of a total length of 3.05 m, a width of 0.41 m and a thickness of 0.41 m. The artificial coal seam in each experiment was prepared from 5 block samples of provided coal which were loaded in the reactor using a chain block hoist and ratchet straps, and then pushed together using a forklift ensuring minimum gap between the blocks (Fig. 3). The total mass of each continuous coal seam used for the experiments was approximately 650 kg (Table 1).
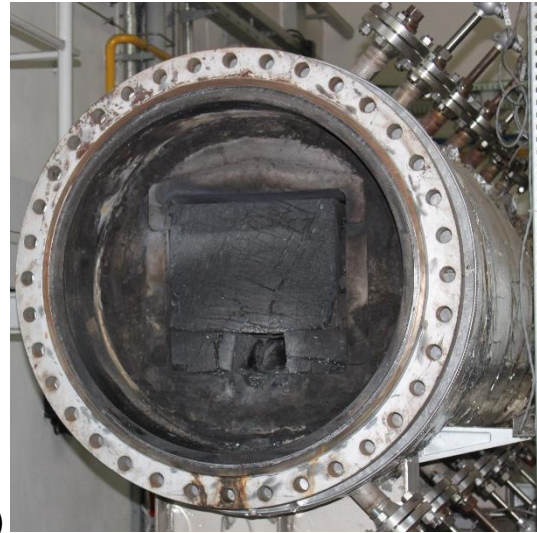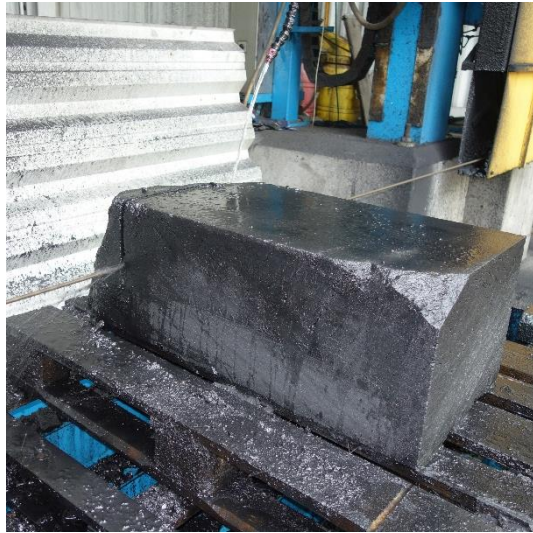
125 **Fig. 3.** Preparation of the artificial coal seams for UCG tests: (a) Coal blocks being processed, (b) The
126 reaction chamber loaded with coal.

127 Table 1. Dimensions and weights of coal blocks used for UCG tests.

Coal block	Width (m)	Height (m)	Length (m)	Weight (kg)
Atmospheric pressure experiment				
1	0.41	0.41	0.73	155
2	0.41	0.41	0.77	163
3	0.41	0.41	0.64	135
4	0.41	0.41	0.26	55
5	0.41	0.41	0.66	140
High-pressure (30 bar) experiment				
1	0.41	0.41	0.35	75
2	0.41	0.41	0.88	187
3	0.41	0.41	0.84	179
4	0.41	0.41	0.62	132
5	0.41	0.41	0.36	77

128 Small pieces of coal were collected from large blocks to be used for coal characterisation which

129 included Proximate and Ultimate analyses, sulphur form analysis and petrographic composition. All

130 analyses were performed by Department of Solid Fuels Quality Assessment of GIG and the results are

131 presented in Table 2. Based on the results obtained and the comparison with the ASTM [30]

132 classification of coal rank, this coal can be classified as semi-anthracite.

133 Table 2. Characteristics of coal used for gasification experiments.

Parameter	Value
As received	
Total moisture (%)	1.15 ± 0.40
Ash (%)	4.61 ± 0.3
Volatiles (%)	9.92 ± 0.12

Total sulphur (%)	1.55 ± 0.04
Calorific value (kJ/kg)	33,416 ± 220
Analytical	
Moisture (%)	0.84 ± 0.30
Ash (%)	4.62 ± 0.3
Volatiles (%)	9.95 ± 0.13
Heat of combustion (kJ/kg)	34,414 ± 228
Calorific value (kJ/kg)	33,527 ± 221
Total sulphur (%)	1.55 ± 0.04
Carbon (%)	87.31 ± 0.66
Hydrogen (%)	3.97 ± 0.28
Nitrogen (%)	1.29 ± 0.12
Oxygen (%)	0.50 ± 0.05
Specific gravity (g/cm^3)	1.35 ± 0.028
Maceral group	
Vitrinite (%)	72 ± 6
Liptinite (%)	0 ± 1
Inertinite (%)	28 ± 3
Vitrinite Reflectance (%)	1.67 ± 0.03
Sulphur form	
Total sulphur (%)	1.55 ± 0.04
Pyritic sulphur (%)	0.75 ± 0.07
Sulphate sulphur (%)	0.05 ± 0.02
Ash sulphur (%)	0.08 ± 0.01
Combustible sulphur (%)	1.47 ± 0.07

134   2.3.   Experimental procedure

135   Two multiday underground coal gasification trials, each lasting 105 hours, were conducted, i.e. one at

136   atmospheric pressure and one at high pressure (30 bar) conditions. The particular stages of the UCG

137   tests are shown in Table 3. Each experiment was divided in six stages, based on the type of gasification

138   reagent and flow rates used. Different stages were considered to assess the impact of various

139   gasification agents on the gas composition and calorific value, as changes in the gasification reagent

140   can be helpful when the gas calorific value decreases as the cavity is growing. Such results can provide

141   initial assessment of the value of the product gas against a particular gasification reagent as different

142   reactants and product gases are associated with specific financial costs/benefits during in-situ

143   gasification. The coal seams were ignited using a pyrotechnic charge located inside the gasification

144   channel at the bottom of the coal seam at a distance of approximately 1 m from the face of the coal

145   seam. The gasification process was started by putting oxygen (99.5% purity) into the ignited coal seam.

146   Upon finishing the experiments, nitrogen was used for extinguishing and cooling down purpose.

147   Table 3. Stages of the underground coal gasification experiments.

Stage	Gasification reagent	Flow rates (Nm^3/h)		Duration (h)
		Atmospheric pressure experiment	High-pressure (30 bar) experiment	
I	Oxygen	5	5	30
II	Oxygen + water	5 (O_2) + 2.5 (H_2O)	5 (O_2) + 2.5 (H_2O)	38
III	Air	6	8	6
IV	Air	10	12	7
V	OEA 50%	5 (air) + 3 (O_2)	7.5 (air) + 4.5 (O_2)	19
VI	OEA 50% + water	5 (air) + 3 (O_2) + 2.5 (H_2O)	7.5 (air) + 4.5 (O_2) + 2.5 (H_2O)	5
Total:				105

148   3. Results and discussion

149   3.1.   Gas production rates

150 The gas production rates as a function of time for the experiments conducted at atmospheric and high

151 pressure (30 bar) are presented in Fig. 4. Overall, the high-pressure experiment provided more stable

152 gas production than the atmospheric one. In particular, during the first stage of gasification using

153 oxygen, the production rate in the atmospheric pressure test was continuously increasing from 7

154 Nm^3/h to 10.9 Nm^3/h, while in the high pressure one it was constant at around 8.3 Nm^3/h. The

155 production rate obtained at atmospheric pressure conditions was then continuously decreasing to 8

156 Nm^3/h, while the change at high-pressure conditions was negligible. Introducing air as a gasification

157 reagent in the third stage did not induce any significant changes in the flow rates obtained at

158 atmospheric pressure conditions, however the flow rates increased up to a maximum of 12.4 Nm^3/h

159 at high-pressure experiment. During the fourth stage, the flow rates obtained in the high-pressure

160 experiment increased to 15 Nm^3/h and remained nearly constant throughout the fifth and sixth stages.

161 For the experiment conducted at atmospheric pressure conditions, the flow rate increased in the

162 fourth stage to 12.6 Nm^3/h, followed by a decline in stage five until reaching 9.1 Nm^3/h and then

163 rebounding to 12.3 Nm^3/h towards the end of the stage. In the sixth stage, a rapid decrease in the

164 flow rates occurred reaching 7.4 Nm^3/h by the end of the experiment. The reason for rapid decline in

165 Stages 5 and 6 is unknown but may be related to the spalling of the gasified material into the

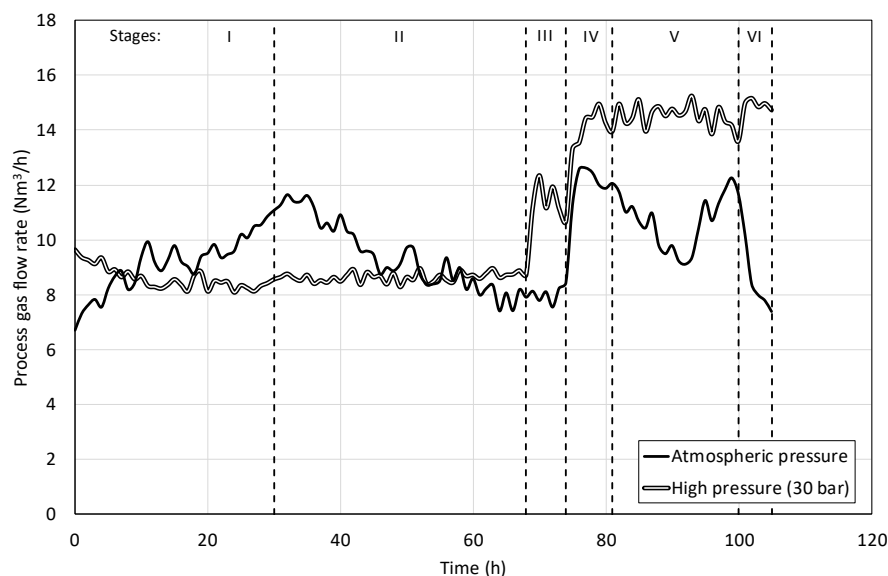166 gasification channel and reducing the gas flow within the reactor.

Fig. 4. Gas production over the course of the atmospheric and high-pressure (30 bar) UCG experiments.

3.2. Gas composition and gas calorific value

Changes in the gas composition obtained over the course of the atmospheric and high-pressure experiments are presented in Fig. 5a and Fig. 5b, respectively. During the 1st stage of both experiments, CH_4 concentration was steadily increasing, opposite to H_2 concentration. However, the 30 bar experiment showed higher rate of CH_4 increase than the atmospheric one. Adding steam to oxygen in the 2nd stage initiated an increase in CH_4 and H_2 concentrations for both atmospheric and 30 bar experiments, yielding maximum concentrations of 6.2% and 20.3% of CH_4 and 27.4% and 17.9% of H_2 by the end of the stage, respectively. Presence of steam benefits H_2 generation through steam gasification and water gas shift reactions which then participates in the hydrogasification and Sabatier reactions favoured at high pressure increasing the production of CH_4. During the 3rd-6th stages of the experiment conducted at atmospheric pressure when air was introduced in the system, CH_4 concentration experienced a steady drop reaching 0.6% by the end of the experiment. For the high-pressure experiment, CH_4 generation was more stable as it decreased to 5.12% during the air gasification stage but then remained nearly constant throughout 4th-6th stages. H_2 generation rapidly decreased at the beginning of the 3rd stage and then slowly increased towards the end of both experiments as more oxygen and steam were added throughout stages 4-6. Generation of CO followed

186   the same pattern as H_2 production in stages 3-6, however the first two stages in both experiments

187   were marked with high CO generation accompanied by high CO_2 concentrations due to strong

188   oxidation reactions initiated by high concentration of O_2 in the reactor. Concentrations of 58.9% and

189   35.1% of CO, and 45.4% and 57.3% of CO_2 were observed in atmospheric and 30 bar experiments,

190   respectively. Injection of air in stages 3-4 decreased the CO_2 generation but increased the N_2 portion

191   in the gas mixture instead, yielding N_2 concentrations in the region of 65-73% in the atmospheric

192   pressure test and 63-68% in the high-pressure test. Small amounts of C_2H_6 and H_2S were measured in

193   both experiments, with the maximum recorded concentrations of 0.37% and 0.84%, and 1.89% and

194   1.35% at the end of the 2nd stage of the atmospheric and high-pressure experiments, respectively.

(a)
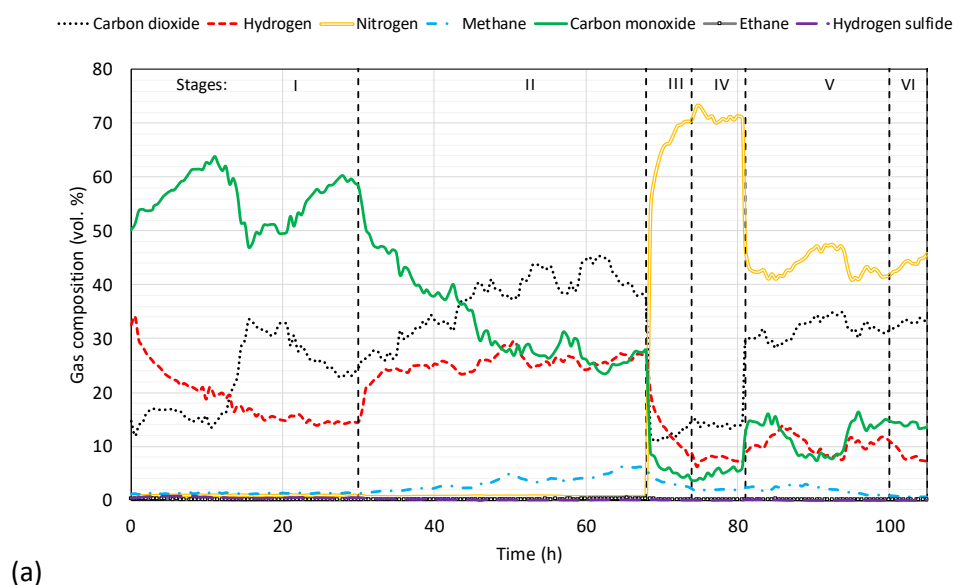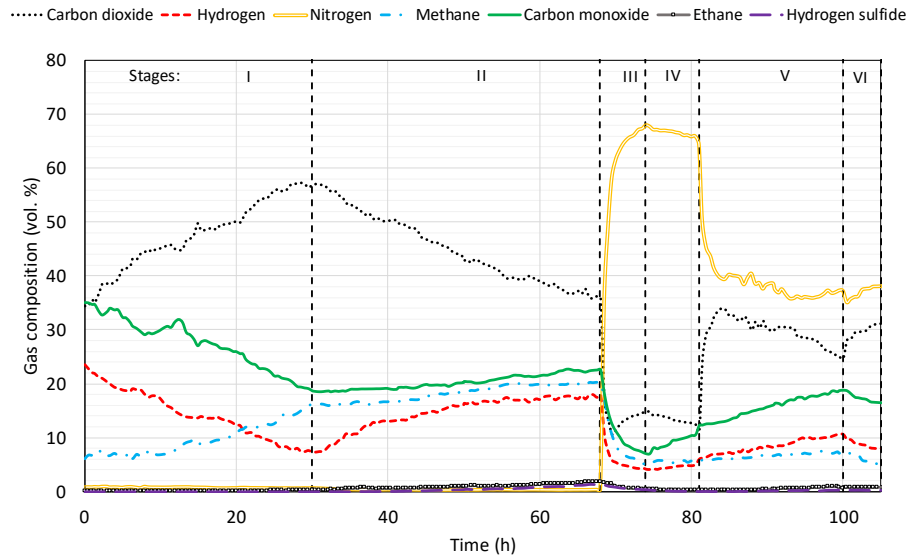
(b)

Fig. 5. Gas composition over the course of the UCG experiments: (a) atmospheric gasification, (b) high-pressure (30 bar) gasification.

Changes in the gas calorific values over the course of both experiments are presented in Fig. 6. As shown for the atmospheric pressure experiment, the maximum gas calorific value of 10.9 MJ/Nm^3 was obtained during the oxygen gasification (the 1st stage). In the subsequent stages, the calorific value of the produced gas has shown a decrease reaching a minimum of 1.8 MJ/Nm^3 during the air gasification (the 3rd and 4th stages). During the high-pressure experiment, the gas calorific value was nearly constant at around 8.6 MJ/Nm^3 in the 1st stage and then steadily increasing throughout the 2nd stage (oxygen and water gasification) reaching a maximum value of 13.52 MJ/Nm^3. During the air gasification, the gas calorific value experienced a sudden drop to a minimum of 3.5 MJ/Nm^3 followed by a recovery with a maximum value of 6.8 MJ/Nm^3 during the OEA gasification.

The changes of gas composition came as a result of several influencing factors such as thermodynamic conditions as well as the composition and temperature of the gasifying agent used. During the oxygen injection, the gasification process is primarily governed by highly exothermic reactions which increase the temperature of the system and produce high concentrations of CO and CO_2. Relatively high concentration of H_2 in the 1st stage can be partially explained through chemical reactions involving an inherent coal moisture. CH_4 production comes primarily as a result of the methanation reaction. However, a relatively high concentration of CH_4 was observed in the high-pressure test compared to

213   the atmospheric pressure test confirming that CH_4 generation is favoured under high pressure

214   conditions. As the water was introduced into the system in the 2nd stage, both the H_2 and CH_4 contents

215   increased, but CO content decreased as a result of the steam gasification and water-gas shift reaction.

216   Consequently, this only improved the gas calorific value in the high-pressure experiment which

217   experienced a more significant increase in the CH_4 content and less reduction in the CO content

218   compared to the atmospheric pressure test. During the air gasification, the gas calorific value reduced

219   significantly as a result of the decrease in the amount of combustible components in the product gas.

220   During the air injection, nitrogen is the main product gas as it does not participate in the main

221   gasification reactions. During the OEA and OEA with water injection, the calorific value of the product

222   gas improves as a result of the increased oxygen content in the reactant gas which increases the

223   temperature in the coal seam and positively affects the gas quality.
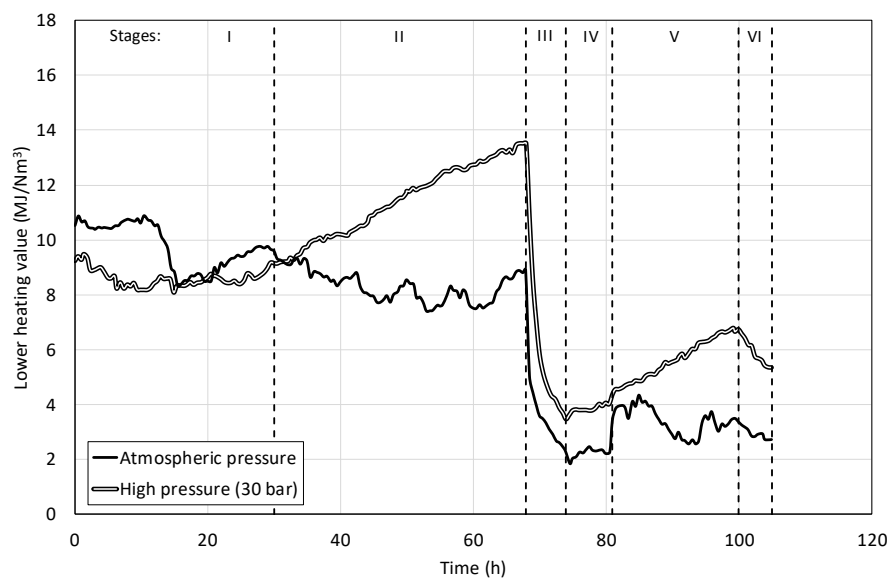
224
225 **Fig. 6.** Changes in gas calorific values over the course of the atmospheric and high-pressure (30 bar)
226 UCG experiments.

227 Table 4 presents the average gas compositions and calorific values obtained during both atmospheric

228 and high-pressure experiments. If the calorific values are compared between the particular stages of

229 each experiment, all stages of the 30 bar experiment except the 1st one result in a higher average

230 calorific value compared to the atmospheric pressure experiment. This exception is related to the

231 rapid development of oxidation zone in the atmospheric gasification which increased the temperature

of the system and enhanced the production of CO and H_2. Overall, the atmospheric test produced

syngas with 18.5% lower average calorific value than the 30 bar experiment which is primarily related

to the higher CH_4 content produced at elevated pressures compared to H_2 and CO.

Table 4. Average gas compositions obtained in the particular stages of the underground coal gasification experiments.

Stage	Gasification reagent	Gas production (Nm³/h)	Average gas composition (%)							Average calorific value (MJ/Nm³)
			CO₂	N₂	H₂	CH₄	CO	C₂H₆	H₂S	
Atmospheric pressure experiment										
I	O₂	9.16	22.43 ±1.12	0.79 ±0.08	18.73 ±0.94	1.27 ±0.06	56.08 ±2.80	0.13 ±0.01	0.57 ±0.06	9.78
II	O₂ + H₂O	9.43	37.01 ±1.85	0.60 ±0.03	25.27 ±1.26	3.40 ±0.17	33.36 ±1.67	0.18 ±0.02	0.18 ±0.02	8.32
III	Air 6 m³/h	8.01	13.47 ±0.67	62.47 ±3.12	13.59 ±0.68	3.34 ±0.17	6.83 ±0.34	0.17 ±0.02	0.13 ±0.01	3.67
IV	Air 10 m³/h	11.87	14.45 ±0.72	70.61 ±3.53	7.66 ±0.38	1.91 ±0.10	5.16 ±0.26	0.14 ±0.01	0.07 ±0.01	2.27
V	OEA 50%	10.67	31.82 ±1.59	43.66 ±2.18	10.50 ±0.53	1.97 ±0.10	11.90 ±0.60	0.07 ±0.01	0.08 ±0.01	3.41
VI	OEA 50% + H₂O	8.79	32.93 ±1.65	43.79 ±2.19	8.48 ±0.42	0.66 ±0.03	14.06 ±0.70	0.03 ±0.01	0.05 ±0.01	2.96
Total:		**9.63**	**28.85 ±1.44**	**18.75 ±0.94**	**18.08 ±0.90**	**2.30 ±0.12**	**31.63 ±1.58**	**0.13 ±0.01**	**0.26 ±0.03**	**6.92**
High pressure (30 bar) experiment										
I	O₂	8.58	43.77 ±2.19	0.65 ±0.06	14.23 ±0.71	9.62 ±0.69	27.50 ±1.38	0.14 ±0.01	<0.05	8.60
II	O₂ + H₂O	8.64	45.11 ±2.26	0.25 ±0.02	14.64 ±0.73	18.26 ±0.91	20.35 ±1.02	0.95 ±0.10	0.44 ±0.04	11.41
III	Air 6 m³/h	11.24	14.50 ±0.73	58.14 ±2.91	6.03 ±0.30	8.82 ±0.44	10.86 ±0.54	0.93 ±0.09	0.72 ±0.07	5.95
IV	Air 10 m³/h	13.90	13.54 ±0.68	66.78 ±3.34	4.55 ±0.23	5.58 ±0.28	9.13 ±0.46	0.27 ±0.03	0.15 ±0.02	3.85
V	OEA 50%	14.53	29.58 ±1.48	38.92 ±1.95	8.45 ±0.42	6.68 ±0.33	15.73 ±0.79	0.49 ±0.05	0.15 ±0.02	5.65
VI	OEA 50% + H₂O	14.83	29.61 ±1.48	36.98 ±1.85	8.77 ±0.44	6.22 ±0.31	17.40 ±0.87	0.75 ±0.08	0.27 ±0.03	5.92
Total:		**10.48**	**38.43 ±1.92**	**16.86 ±0.84**	**11.97 ±0.60**	**11.77 ±0.59**	**20.14 ±1.01**	**0.58 ±0.06**	**0.25 ±0.03**	**8.49**

Fig. 7 presents the experimental data provided in the literature on the gas calorific values obtained

during gasification of coals of different rank using air, OEA and oxygen [19, 21, 23, 26, 27] and the

comparison with the gas calorific values calculated as a part of this study. Comparing each result

provided in regard to air gasification, the gas calorific value generally increases with the total carbon

content in coal, but no precise interdependency can be established as gasification at high pressures

involved higher air flow rates. The gas calorific values obtained during OEA gasification do not show a

clear relationship with the total carbon content of coal. This is mainly due to the fact that in each

experiment reported in the literature, different ratios of oxygen to air were used. Nevertheless, it can

245 be observed in Fig. 7 that the gas calorific values obtained during the OEA gasification as reported in

246 the literature and in this work are generally higher than the values obtained during the air gasification.

247 In case of oxygen gasification, the values presented in Fig. 7 show that there is a clear increase in the

248 gas calorific values with an increase in coal rank. In particular, gasification of semi-anthracite at

249 atmospheric conditions as shown in this work can produce a syngas with 2.8 times higher calorific

250 value than gasification of lignite coal [19]. In comparison to the bituminous coal [26], an increase of

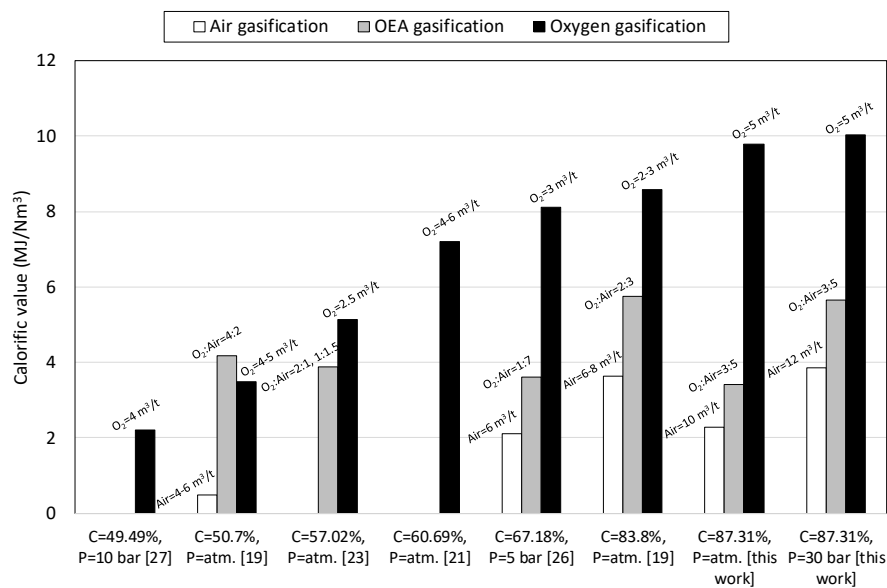251 21% in calorific value is observed.

252

253 **Fig. 7.** Gas calorific values obtained during gasification of coals of different rank using air, OEA and
254 oxygen as reported in the literature and comparison with the results obtained in this work. Values
255 above the bars specify flow rates of oxygen and air, and oxygen to air ratios used in the OEA
256 experiments.

257 3.3. Temperature distribution

258 The variations of temperature inside the reactor next to the gasification channel for the atmospheric

259 and high-pressure experiments are given in Fig. 8a and 8b, respectively. While the temperatures

260 recorded by T3-T6 are similar for both experiments, different temperatures between the experiments

261 were experienced by thermocouple T2 which was in the proximity of the injection point. In particular,

262 the highest temperatures recorded were 1246°C and 1076°C in the atmospheric and high-pressure

263 experiments, respectively. Such variation may be attributed to the difference in total rates of oxidation

264 reactions, both complete and partial, with carbon. In general, coal combustion reaction phenomena

265   is affected by a number of factors such as coal porosity and its distribution, coal particle size, types

266   and contents of specific mineral matter as well as heat and mass transfer conditions in the reactor

267   [31]. Such reactions are highly exothermic and consequently, the ratio of the primary products, CO to

268   CO_2, sharply increases with increasing temperature [31]. Values presented in Table 4 confirm this

269   phenomenon as the ratio of CO to CO_2 was 2.5 for the atmospheric gasification compared to the ratio

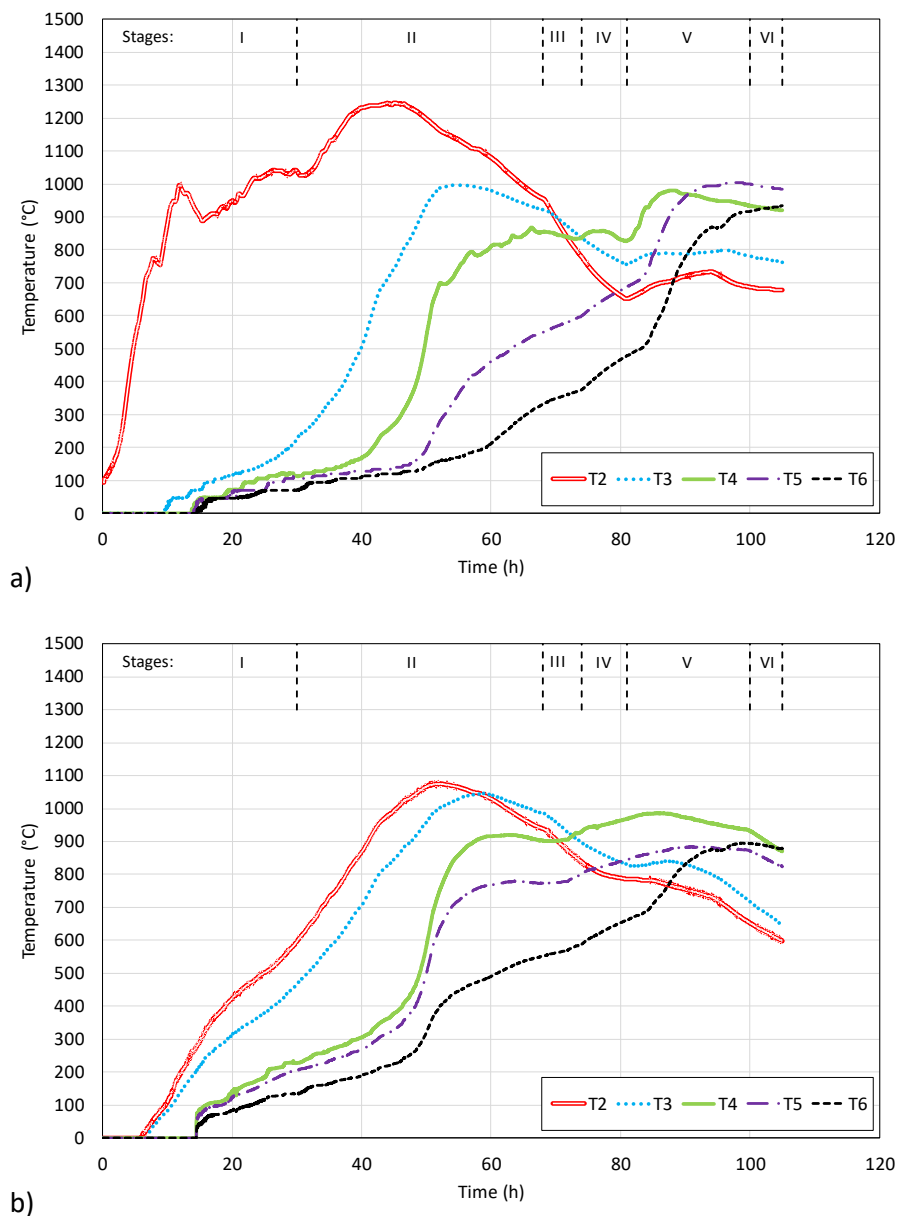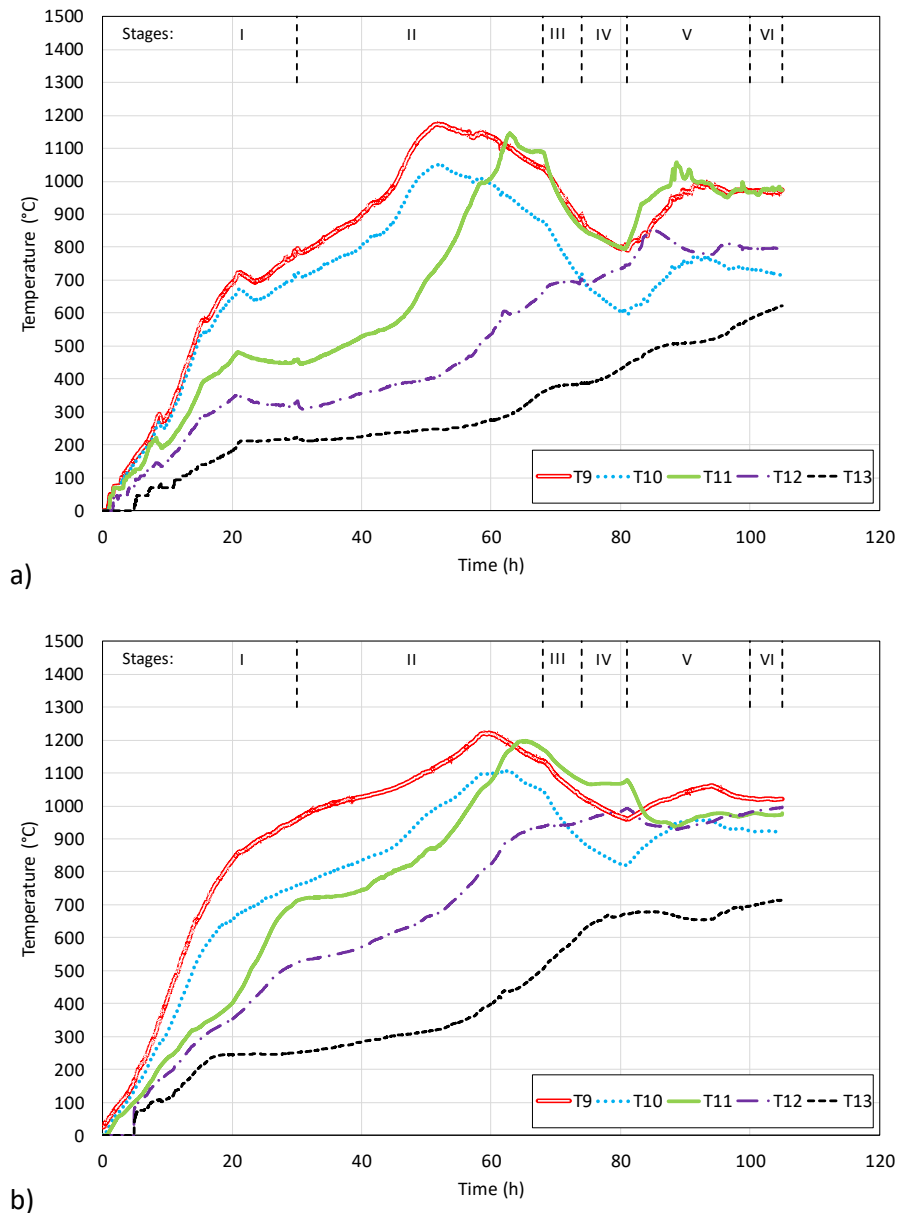270   of 0.6 for the 30 bar experiment.

a)

b)

271   **Fig. 8.** Temperature distributions in the gasification channel over the course of the UCG experiments:
272   a) atmospheric gasification, b) high-pressure (30 bar) gasification.

273   The temperature evolutions in the roof of the strata are given in Fig. 9a for the atmospheric pressure

274   experiment and in Fig. 9b for the high-pressure experiment. Similar to the temperature measurements

275   in the gasification channel, the maximum temperatures in the roof strata were recorded 0.5 m from

276   the injection face of the coal seam. However, the temperature of 1222°C recorded in the high-pressure

277   experiment was slightly higher than the 1174°C recorded in the atmospheric pressure experiment.

a)

b)

278   **Fig. 9.** Temperature distributions in the roof strata over the course of the UCG experiments: a)
279   atmospheric gasification, b) high-pressure (30 bar) gasification.

280   On average in both experiments, the highest temperatures at 0.5 m, 1.0 m and 1.5 m from the

281   injection face of the coal seam were recorded during the 2nd stage (oxygen and water gasification)

282 followed by a decrease during the air gasification and a slight recovery during the gasification with

283 OEA and OEA with water. Temperatures at 2.0 m and 2.5 m from the gas inlet in the roof strata showed

284 a continuous increase over the experiment reaching a maximum during the OEA gasification.

285 ### 3.4. Process balance data

286 Based on the experimental data presented earlier, Table 5 shows calculated values of average

287 gasification rates, energy efficiency and average reactor power for particular stages.

288 The 1st stage of the atmospheric pressure experiment showed a higher efficiency of 58.35% than the

289 2nd stage exhibiting 54.25%, which was the opposite for the high-pressure experiment which showed

290 an efficiency of 48.56% in the 1st stage and 64.08% in the second stage. During air gasification (the 3rd

291 and 4th stages), there was surprisingly an increase in the process energy efficiency up to 73.20% in the

292 atmospheric pressure test and 79.36% in the high-pressure test, despite the decrease in the gas

293 calorific values. This can be attributed to the relatively short duration of the air gasification stages (13

294 hours in total) as well as the accumulated thermal energy from the 2nd stage. Similar to the first two

295 stages, the gasification with OEA under atmospheric pressure conditions showed higher efficiency

296 (35.83%) than the gasification with OEA and water (30.29%). The opposite was observed in the high-

297 pressure experiment, where the OEA and water yielded a higher energy efficiency (52.10%) than the

298 OEA gasification (51.21%). In total, energy efficiency of the gasification at 30 bar is 57.67% which is

299 higher compared to the atmospheric pressure gasification efficiency of 51.72%.

300 Table 5. Mass and energy balance calculations for particular stages of the underground coal
301 gasification experiments.

Stage	Gasification reagent	Total gas yield (Nm3)	Energy in process gas (MJ)	Average reactor power (kW)	Gasification rate (kg/h)	Energy in coal consumed (MJ)	Energy efficiency (%)
Atmospheric pressure experiment							
I	Oxygen	274.64	2670.70	24.73	4.51	4576.84	58.35
II	Oxygen + water	358.24	2999.80	21.96	4.30	5529.81	54.25
III	Air 6 m³/h	48.06	175.67	8.14	1.18	239.98	73.20
IV	Air 10 m³/h	83.06	190.32	7.48	1.59	377.04	50.48
V	OEA 50%	202.77	693.31	10.15	3.01	1935.07	35.83

VI	OEA 50% + water	43.94	132.22	7.30	2.58	436.53	30.29
Total:		1010.68	6862.02	18.15	3.37	1326.97	51.72
High-pressure (30 bar) experiment							
I	Oxygen	257.51	2219.08	20.48	4.50	4569.79	48.56
II	Oxygen + water	328.22	3750.84	27.42	4.55	5853.49	64.08
III	Air 8 m³/h	67.45	401.64	18.59	2.49	506.11	79.36
IV	Air 12 m³/h	97.32	378.07	15.02	2.46	583.31	64.80
V	OEA 50%	276.14	1559.49	22.80	4.74	3045.03	51.21
VI	OEA 50% + water	74.15	440.26	24.46	5.02	845.04	52.10
Total:		1100.79	8449.31	23.15	4.34	15402.76	57.67

4. Conclusions

The experiments conducted demonstrated a significant influence of the gasifying medium used and applied pressure regime (atmospheric pressure and 30 bar pressure gasification) on the UCG gas composition and overall process efficiency. Hence, the following conclusions can be made:

- Although the gas from the gasification process at 30 bar using O_2 as a reactant contained more CH_4 compared to the atmospheric pressure gasification, as the methanation and hydrogasification reactions are favoured at high pressures, it contained less H_2 and CO leading to slightly lower calorific value in the 30 bar experiment. This was mainly attributed to the higher temperature near the reactor inlet during atmospheric gasification, caused by variations in total rates of oxidation reactions and benefiting Boudouard, gas-shift and steam gasification reactions to enhance the production of H_2, CO and CO_2.

- Injection of water in the 2nd stage led to a decrease in CO content and an increase in the content of CO_2, H_2 and CH_4 in both experiments, however, the observed changes were more pronounced for the high-pressure process.

- During the air gasification stages, an increase in the process energy efficiency was observed compared to previous stages with oxygen and water, although the gas caloric value decreased in both experiments. Injection of OEA and adding water to it subsequently resulted in improvement of gas quality but reduced the gasification efficiency in both experiments. However, if the results are calculated on a N_2-free basis, one could infer that the gas calorific

321   value of air gasification stages are similar, or even higher for the 30 bar gasification, to both

322   the stages where oxygen and OEA were injected. Such behaviour can be attributed to the

323   relatively short duration of the air gasification stages and the fact that the reactor had an

324   accumulated thermal energy from the stages where oxygen was the main reactant.

325   • The overall energy efficiency of the high pressure (30 bar) experiment was higher compared

326   to the atmospheric pressure test, i.e. 57.67% compared to 51.72%. This was mainly due to

327   higher methane concentrations in gas obtained during the high-pressure experiment.

328   • Under elevated pressure, the temperatures recorded in the roof strata were higher compared

329   to the atmospheric gasification, while the opposite was observed in the gasification channel.

330   The differences may have resulted from different total rates of oxidation reactions and

331   variations in fluid flow patterns in the gasification chamber during the two experiments, which

332   influenced the heat transport due to convection. Additionally, heat insulating effects of coal

333   ash remaining in the gasification channel could take place. The distribution of ash strongly

334   depends on the fluid flow conditions in the reaction chamber and on the distribution of ash in

335   the raw coal sample.

336   • By comparing the results of this work with the available literature data, it can be concluded

337   that there is an increase in the gas calorific values with an increase in coal rank, as syngas with

338   more than 280% and 20% higher calorific value can be obtained by gasification of semi-

339   anthracite compared to lignite and bituminous coals, respectively.

340   • The conditions simulated in the reactor are similar to those during the Linked Vertical Wells

341   (LVW) process. As a consequence, a gradual deterioration of the gas quality is observed during

342   the experiments. This resulted in the elaboration of CRIP technique, in which a new reactor is

343   started when the gas quality decreases. The obtained results suggest that the proper

344   manipulation in reactant dosing may practically help in more stable gas quality in CRIP as well

345   as in LVW technique. In those techniques the gas calorific value decreases as the cavity is

346   growing so to counteract such phenomenon, the changes in the gasification reagent could be

347   helpful. It is extremely important not to exceed the hydrostatic pressure of the surrounding

348   to avoid pressure losses and gas leakages.

349   • The main factors influencing the gas composition are the gasification reagent used and long-

350   term stability of the gasification conditions. In order to obtain stable syngas quality in terms

351   of its calorific value, it is important to provide an appropriate amount of oxidant to the reactor.

352   The best reagent to obtain a high calorific gas during UCG is the mixture of oxygen and water

353   unless natural water is available in excess quantities. A gradual decrease in the gas calorific

354   value, however, cannot be avoided during operation of a single reactor, so retracting the

355   oxygen injection point (CRIP technique) would be necessary to maintain the process at the

356   desired parameters.

5. Acknowledgements

6. References

362   1.   IPCC. The Intergovernmental Panel on Climate Change, *Global warming of 1.5°C. An IPCC*
363   *Special Report.* 2018.
364   2.   The Royal Society and Royal Academy of Engineering, *Greenhouse gas removal.* Report, 2018.
365   3.   International Energy Agency (IEA), *World Energy Outlook 2018.* 2018.
366   4.   International Energy Agency (IEA). *Carbon Capture and Storage: The solution for deep*
367   *emissions reductions*. 2015. IEA.
368   5.   Shafirovich, E. and A. Varma, *Underground coal gasification: a brief review of current status.*
369   Industrial & Engineering Chemistry Research, 2009. **48**(17): p. 7865-7875.
370   6.   Thomas, H., et al. *Deep Ground and Energy: Carbon Sequestration and Coal Gasification*. in
371   *The International Congress on Environmental Geotechnics*. 2018. Springer.
372   7.   Bhutto, A.W., A.A. Bazmi, and G. Zahedi, *Underground coal gasification: From fundamentals*
373   *to applications.* Progress in Energy and Combustion Science, 2013. **39**(1): p. 189-214.
374   8.   Perkins, G., *Underground coal gasification–Part I: Field demonstrations and process*
375   *performance.* Progress in Energy and Combustion Science, 2018. **67**: p. 158-187.
376   9.   Wang, F., *Comparison of analytical methods for phenols, cyanide, and sulfate as applied to*
377   *groundwater samples from underground coal gasification sites*, in *Analysis of Waters*
378   *Associated with Alternative Fuel Production*. 1980, ASTM International.
379   10.   Thorsness, C. and J. Britten, *Lawrence Livermore National Laboratory Underground Coal*
380   *Gasification project*. 1989, Lawrence Livermore National Lab., CA (USA).

381 11. Dennis, D., *Rocky Mountain 1 underground coal gasification test project Hanna*. 2006,
382   Wyoming, Final technical report for the Period 1986 to 2006. National Energy Technology
383   Laboratory.
384 12. Chandelle, V., et al. *Overview about Thulin Field Test*. in *Proceedings of the Twelfth Annual
385   Underground Coal Gasification Symposium, Saarbrucken, Germany*. 1986.
386 13. Chappell, B. and M. Mostade. *The El Tremedal underground coal gasification field test in
387   Spain–First trial at great depth and high pressure*. in *Fifteenth annual international Pittsburgh
388   coal conference*. 1998.
389 14. Wiatowski, M., et al., *Technological aspects of underground coal gasification in the
390   Experimental "Barbara" Mine.* Fuel, 2015. **159**: p. 454-462.
391 15. Mao, F., *Underground coal gasification (UCG): a new trend of supply-side economics of fossil
392   fuels.* Natural Gas Industry B, 2016. **3**(4): p. 312-322.
393 16. Blinderman, M. and R. Jones. *The Chinchilla IGCC project to date: Underground coal
394   gasification and environment*. in *Proceedings of the Gasification Technologies Conference, San
395   Francisco, CA, USA*. 2002.
396 17. Olness, D., *The Angrenskaya underground coal gasification station*. Vol. 53300. 1982:
397   Lawrence Livermore Laboratory.
398 18. Stańczyk, K., et al., *Dynamic experimental simulation of hydrogen oriented underground
399   gasification of lignite.* Fuel, 2010. **89**(11): p. 3307-3314.
400 19. Stańczyk, K., et al., *Gasification of lignite and hard coal with air and oxygen enriched air in a
401   pilot scale ex situ reactor for underground gasification.* Fuel, 2011. **90**(5): p. 1953-1962.
402 20. Stańczyk, K., et al., *Experimental simulation of hard coal underground gasification for
403   hydrogen production.* Fuel, 2012. **91**(1): p. 40-50.
404 21. Kapusta, K., M. Wiatowski, and K. Stańczyk, *An experimental ex-situ study of the suitability of
405   a high moisture ortho-lignite for underground coal gasification (UCG) process.* Fuel, 2016. **179**:
406   p. 150-155.
407 22. Laciak, M., et al., *The analysis of the underground coal gasification in experimental equipment.*
408   Energy, 2016. **114**: p. 332-343.
409 23. Gur, M., et al., *Experimental results of underground coal gasification of Turkish lignite in an
410   ex-situ reactor.* Fuel, 2017. **203**: p. 997-1006.
411 24. Wang, Z., et al., *Expansion of three reaction zones during underground coal gasification with
412   free and percolation channels.* Fuel, 2017. **190**: p. 435-443.
413 25. Su, F.-q., et al., *Evaluation of a Compact Coaxial Underground Coal Gasification System Inside
414   an Artificial Coal Seam.* Energies, 2018. **11**(4): p. 898.
415 26. Wiatowski, M., et al., *Ex-situ experimental simulation of hard coal underground gasification at
416   elevated pressure.* Fuel, 2016. **184**: p. 401-408.
417 27. Wiatowski, M., et al., *Efficiency assessment of underground gasification of ortho-and meta-
418   lignite: High-pressure ex situ experimental simulations.* Fuel, 2019. **236**: p. 221-227.
419 28. Konstantinou, E. and R. Marsh, *Experimental study on the impact of reactant gas pressure in
420   the conversion of coal char to combustible gas products in the context of Underground Coal
421   Gasification.* Fuel, 2015. **159**: p. 508-518.
422 29. Sadasivam, S., et al., *Experimental study of methane-oriented gasification of semi-anthracite
423   and bituminous coals using oxygen and steam in the context of underground coal gasification
424   (UCG): Effects of pressure, temperature, gasification reactant supply rates and coal rank.* Fuel,
425   2020. **268**: p. 117330.
426 30. ASTM Standards, *ASTM D388. Standard Classification of Coals by Rank.* ASTM International,
427   2015. **05.06**(West Conshohocken, PA).
428 31. Lee, S., J.G. Speight, and S.K. Loyalka, *Handbook of alternative fuel technologies*. 2014: crc
429   Press.

430